KENNETH R. ALLEN and RICHARD I. JOSEPH

A STATISTICAL MECHANICAL EXPLANATION OF THE GARRETT AND MUNK MODEL OF OCEANIC INTERNAL WAVES

Although the Garrett and Munk model of oceanic internal waves provides a useful catalog of existing ocean measurements, it is empirical and does not explain the observed spectra theoretically. By using methods from statistical mechanics, however, a first-principles understanding of the Garrett and Munk model can be obtained.

Editor's note: *It is probably not a coincidence that ocean waves, both surface and internal, have equilibrium energy spectra that are global. By global spectra we mean that the distribution of wave amplitudes among the various frequencies appears to be similar no matter where the waves are measured (avoiding pathological situations). To a scientist conversant with statistical mechanics, this finding suggests the existence of underlying variables that are canonical, with energy states that are exponentially distributed, much like the molecules of a gas immersed in a constant-temperature bath. In this highly theoretical article, Allen and Joseph show that for oceanic internal waves, statistical equilibration is apparent. The methods of statistical mechanics are applied to weakly interacting internal waves by using the less often used Lagrangian description of fluid dynamics (in contrast with the normal Eulerian description). The authors use these methods, along with the assumptions of a canonical distribution and the existence of a total energy level E_0 analogous to, but most certainly not, the thermal energy kT. From this first-principles calculation is derived the Garrett–Munk energy spectrum—a semi-empirical but globally observed internal wave distribution. The authors then show that the Garrett–Munk spectrum is not a fundamental property of the system, as is a Maxwellian velocity distribution for a gas, but rather is partly a consequence of the measurement process used to observe internal waves. The underlying canonical spectrum is presented, and various projections of it are given. More recently, Allen and Joseph have applied the same methods to ocean surface waves and have obtained the observed global equilibrium wave-vector spectrum in the saturation region of large wave numbers. Their demonstration of statistical equilibration is philosophically satisfying and is believed to be very important in the deeper understanding of geophysical fluid dynamics.*

J. R. Apel

INTRODUCTION

Almost two decades have passed since Garrett and Munk[1,2] introduced the model variance spectrum, which is now referred to as the GM model. They were concerned with the various fluctuation spectra associated with oceanic temperature and velocity fields at length scales and time scales typically ascribed to internal waves. As an example, Figure 1 shows a typical moored vertical-displacement spectrum, replotted from the results of Cairns and Williams,[3] corresponding to a moored experiment conducted at a depth of about 350 m some 800 km offshore of San Diego, Calif. The moored spectrum is a function of frequency ω, exhibits an ω^{-2} decay, and for the most part lies between the inertial frequency f and the Väisälä frequency N (f and N will be discussed in more detail later). Figure 2 is a typical example of a horizontal tow spectrum, replotted from the results of Katz,[4] that corresponds to a towed experiment conducted in the Sargasso Sea at a depth of between 700 and 800 m. The tow spectrum is a function of horizontal wave number κ and typically exhibits a decay between κ^{-2} and κ^{-3}. The GM model assumes that these fields are due to a random superposition of linear internal waves, and the amplitudes of the waves are empirically adjusted to obtain agreement between the model and the various spectra associated with the observed fields. Although the GM model provides a useful and surprisingly reliable catalog of existing experiments, it is empirical and does not explain the various
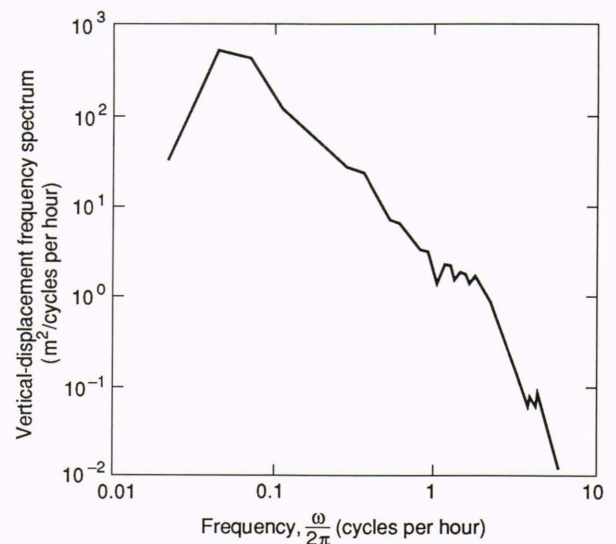
Figure 1. A typical moored vertical-displacement spectrum. (Adapted from Ref. 3.)
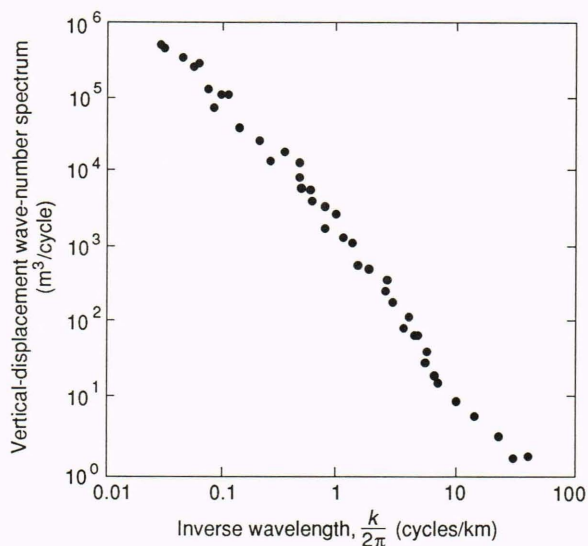
Figure 2. A typical vertical-displacement horizontal tow spectrum. (Adapted from Ref. 4.)

observed spectra theoretically. In this article, we will examine the issue of how far one can go in obtaining a first-principles understanding of the GM model and will discuss some recent theoretical developments[5,6] that play an important role in providing such an explanation. We will show that by applying the methods of statistical mechanics to the problem of calculating the various fluctuation spectra observed in the ocean, this goal can be attained.

In developing such a theory, it is important to distinguish carefully between Lagrangian and Eulerian variables. Most observations and empirical studies are in terms of Eulerian variables, whereas the methods of statistical mechanics that will ultimately be useful for understanding and interpreting these studies are in terms of Lagrangian variables. This situation raises the issue of how to relate calculated statistical quantities, such as spectra, to the corresponding measured quantity given in terms of Eulerian variables. In a Lagrangian formulation, the fluid is divided into microscopically large, but macroscopically small, parcels that are identified by the various values of a three-dimensional parameter that we will denote by the vector r. We will follow the usual custom that r corresponds to the position of the parcel under the reference condition taken to be the undisturbed or static condition. Once selected, a specific value for r remains with the fluid parcel and does not change throughout the dynamic evolution of the system. We will denote the Lagrangian displacement by $s_L(r, t)$ and the Lagrangian velocity by $v_L(r, t)$, where t is time. In addition, we will denote the Eulerian displacement by $s_E(x, t)$ and the Eulerian velocity by $v_E(x, t)$, where a given value for the Eulerian label x corresponds to a specific point in space and refers to the fluid parcel that happens to be at that point at time t. Thus, a given value for the Eulerian label x does not always refer to the same fluid parcel. The difference between these two labeling systems plays an important role in developing

a first-principles explanation for the observed oceanic spectra.

The difficulty in relating the two sets of variables is that the exact transformation between them is generally not tractable. It was recently shown, however, that a class of systems exists for which the problem of implementing an exact transformation can be avoided, and yet a tractable relation between Lagrangian and Eulerian spectra can be obtained.[5,6] It was shown that over at least part of the wave-number domain, the Lagrangian and Eulerian wave-number spectra are significantly different. The calculated moored frequency spectra are dominated by small wave numbers, where the Lagrangian and Eulerian spectra are found to be approximately equal, and are in good agreement with experimental spectra, such as the one shown in Figure 1 (a precise definition of large and small wave numbers will be given later). Most tow experiments are concerned with large wave numbers, however, and at large wave numbers independent of the large wave-number structure of the Lagrangian spectra, the Eulerian wave-number spectra exhibit a power-law decay in excellent qualitative agreement with experimental spectra, such as the one shown in Figure 2. This large wave-number power-law decay is strictly a kinematic effect due to advection and is independent of the detailed structure of the Lagrangian spectra. It is important to account for this effect, however, when comparing theoretical calculations with experiment.

We will first briefly discuss the empirical GM model and define the four-dimensional Eulerian frequency-wave-number spectra. These spectra are determined by the distribution of linear internal-wave amplitudes in frequency ω and in the three-dimensional wave vector k. We will then outline the development of a fundamental theory in terms of Lagrangian variables and define the four-dimensional Lagrangian frequency–wave-number spectra. We will show that the four-dimensional Lagrangian frequency–wave-number spectra, rather than the corresponding Eulerian spectra, are fundamentally related to the distribution of energy among the linear internal-wave modes. Next, we will define the Eulerian variables in terms of the Lagrangian variables and obtain an expression for the four-dimensional Eulerian frequency-wave-number spectra in terms of the corresponding Lagrangian spectra. It will become clear that, in general, the two types of spectra are significantly different. We will then present a comparison between theory and experiment for a variety of marginal Eulerian spectra and demonstrate that striking agreement can be obtained. Most important, we will then discuss the implications of the theory and make some suggestions for future theoretical and experimental investigations.

THE GM MODEL

The GM model uses Eulerian variables and assumes that the observed fields are due to a random superposition of linear internal waves. The Eulerian displacement can be written in the form

LAGRANGIAN VERSUS EULERIAN VARIABLES

Because the relation between Lagrangian and Eulerian variables plays such a crucial role in the development of our theory, we provide this thumbnail sketch of the important differences between Lagrangian and Eulerian variables. In the figure, the box labeled *r* depicts a fluid parcel (particle) at its undisturbed position *r*. The box labeled *x* depicts the same fluid parcel when it has been displaced a distance *s* to the new position *x*. The two methods of labeling the displacement are shown in the figure. Because Lagrangian and Eulerian variables both describe the same displacement, they are equal; only the labeling system is different. The different labeling system, however, leads to profound differences in the behavior of the variables.

$$s = s_L (r, t) = s_E (x, t)$$

$$x = r + s_L (r, t) = r + s_E (x, t)$$
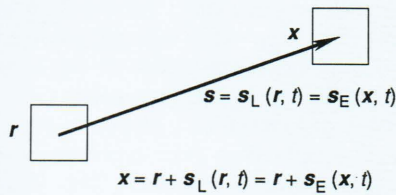
The relation between Lagrangian and Eulerian variables.

Newton's second law describes the relation between the acceleration of a specific particle and the forces that act upon it. Thus, it is the Lagrangian variables that must be used in Newton's laws, and we may write

$$F = ma_L \ ,$$

where F is the force, m is the mass, and a_L is the Lagrangian acceleration. The Lagrangian acceleration is simply $a_L = \partial v_L / \partial t$, so the Lagrangian equations of motion take the form

$$\frac{\partial v_L (r,t)}{\partial t} = \frac{F}{m} \ .$$

The Eulerian velocity changes because forces act upon the fluid parcel and because new fluid with a different velocity can move to the point *x*. The second type of change is referred to as advection and must be accounted for in the Eulerian equations of motion. Thus, the Eulerian equations of motion take the form

$$\frac{\partial v_E (x, \ t)}{\partial t} + [v_E (x, \ t) \cdot \nabla]v_E(x, \ t) = \frac{F}{m} \ .$$

The additional nonlinear term $[v_E(x, \ t) \cdot \nabla]v_E(x, \ t)$ accounts for the flow of fluid into and out of the region around *x* and makes the Eulerian equations of motion fundamentally more complicated than the corresponding Lagrangian equations of motion. The true dynamics of the system evolution is driven by the term F/m, which contains linear forces and what we refer to as the dynamic nonlinearities.

A considerable effort in statistical mechanics has been devoted to understanding the statistical distribution of the Lagrangian variables because the usual formulations of Newton's laws (e.g., Hamilton's canonical equations) have been in terms of these variables. A significant historical precedent exists for the assumption that the statistical distribution of Lagrangian variables is Gaussian: The well-known Maxwell–Boltzmann velocity distribution describes a Gaussian distribution of Lagrangian (i.e., particle) velocities. Further, many studies in statistical mechanics have established the relationship between the dynamic nonlinearities and the evolution of the system to a Gaussian distribution in terms of Lagrangian variables. No corresponding demonstrations exist for Eulerian variables, except for the special case in which the Lagrangian and Eulerian variables are approximately equal. In the theory presented here, we assume that the Lagrangian variables show a Gaussian distribution and then compute the Eulerian statistical quantities by transforming from the Lagrangian to the Eulerian frame.

$$s_E(x, \ t) = \sum_{j=-M}^{M} \frac{1}{(2V\rho\Omega_j)^{\frac{1}{2}}}$$
$$\times \left[\left(\frac{l_{jh}}{l_j} \ \hat{x}_3 - \frac{l_{j3}}{l_j} \ \hat{l}_{jh} \right) a_j (t) - \frac{fl_{j3}}{\Omega_j l_j} \ \hat{n}_j b_j (t) \right]$$
$$\times \exp(il_j \cdot x) \ , \tag{1}$$

where $a_j(t)$ and $b_j(t)$ are complex linear internal-wave amplitudes, Ω_j is the eigenfrequency associated with the *j*th linear internal wave, and $2M + 1$ is the number of degrees of freedom (i.e., the number of individual internal-wave modes included), which will later be allowed to become arbitrarily large. In Equation 1, the various parameters have been chosen such that l_j is a three-dimensional wave vector of magnitude l_j, l_{jh} is the horizontal component of l_j, l_{jh} is the magnitude of l_{jh}, $\hat{l}_{jh}$ is a unit vector in the direction of l_{jh}, l_{j3} is the vertical component of l_j, $\hat{x}_3$ is a vertical unit vector, the

unit vector $\hat{n}_j = \hat{x}_3 \times \hat{l}_{jh}$, ρ is the fluid density, and V is the volume of the ocean that is finite for now but will later be allowed to become arbitrarily large. In writing Equation 1, we have set the Väisälä profile equal to the constant N, assumed that the Coriolis vector f is vertical, and used periodic boundary conditions in the vertical and horizontal directions. Under these conditions, the dispersion relation is given by

$$\Omega_j = \frac{(N^2 l_{jh}^2 + f^2 l_{j3}^2)^{\frac{1}{2}}}{l_j} \ . \tag{2}$$

The expressions given by Equations 1 and 2 are well-known in the theory of linear internal waves, and other detailed treatments can be found elsewhere.[7,8] Because our purpose in this article is to focus on fundamental issues, we will make as many simplifying assumptions as possible. We will find later that obtaining the best agreement between theory and experiment requires a more realistic surface-boundary condition. Although it

is straightforward to incorporate this condition as well as a more realistic Väisälä profile, they only affect details; to include them now would complicate the mathematics, obscure the physics, and add nothing of fundamental importance.

In the linear theory, the complex amplitudes can be written as

$$a_j(t) = a_j \cos(\Omega_j t) + b_j \sin(\Omega_j t) \; , \qquad (3a)$$

and

$$b_j(t) = b_j \cos(\Omega_j t) - a_j \sin(\Omega_j t) \; , \qquad (3b)$$

where a_j and b_j are complex initial values. The vertical component of l_j is given by a positive or negative integer multiplied by $2\pi/D$, where D is the depth of the ocean, and the horizontal components of l_j are given by positive or negative integers multiplied by $2\pi/A^{1/2}$, where A is the surface area of the ocean. We will designate the labeling system such that $l_{-j} = -l_j$. Because the displacement must be real, it is clear from Equations 1 through 3 that we must require that $a_{-j}(t) = a_j^*(t)$ and $b_{-j}(t) = b_j^*(t)$, and that the initial values also satisfy the same conditions. Because of these conditions, the complex amplitudes associated with a given negative value of j are not independent of those associated with the corresponding positive value of j. If we write the complex amplitudes in terms of their real and imaginary parts such that $a_j(t) = a_{j1}(t) + ia_{j2}(t)$ and $b_j(t) = b_{j1}(t) + ib_{j2}(t)$, then $a_{jm}(t)$ and $b_{jm}(t)$ ($1 \le j \le M, 1 \le m \le 2$) are real, independent amplitudes. To completely specify the amplitudes, the initial values for all of the a_{jm} and b_{jm} must be specified.

The essence of the GM model is the specification of the initial values a_{jm} and b_{jm} as random Gaussian variables that are described by the probability density function $g_E(a, b)$ given by

$$g_E(a, b) = \prod_{j=1}^{M} \prod_{m=1}^{2} \frac{\Omega_j}{2\pi\Lambda_{Ej}}$$

$$\times \exp\left[-\frac{\Omega_j}{2\Lambda_{Ej}} (a_{jm}^2 + b_{jm}^2) \right] \; , \quad (4)$$

where Λ_{Ej} is the Eulerian energy distribution, which is empirically specified by GM. Once the probability density $g_E(a, b)$ has been specified, it is straightforward to compute any of the various correlation functions and spectra of interest. The expectation value $E[F_E(a, b, t)]$ of any function $F_E(a, b, t)$ of the Eulerian initial values and time is given by

$$E[F_E(a, b, t)] = \int F_E(a, b, t) g_E(a, b)$$

$$\times \prod_{j=1}^{M} \prod_{m=1}^{2} da_{jm} \, db_{jm} \; , \qquad (5)$$

where, unless otherwise noted, all integrals are over the full range of the integration variable. The various Eulerian displacement correlation functions $C_{Es\alpha\beta}(X, \tau)$ are defined by

$$C_{Es\alpha\beta}(X, \tau) = E[s_{E\alpha}(x + X, t + \tau)s_{E\beta}(x, t)] \; , \; (6)$$

where α and β denote the Cartesian coordinates of the displacement. We will illustrate this development by considering the correlation function associated with vertical displacement. By using Equation 1 and Equations 3 through 6, we find

$$C_{Es33}(X, \tau) = \frac{1}{(2\pi)^3 \rho} \int \frac{l_h^2 \Lambda_E(l)}{l^2 \Omega^2(l)}$$

$$\times \cos[\Omega(l)\tau]\cos(l \cdot X) \, d^3 l \; , \quad (7)$$

where we took the limit that V becomes arbitrarily large so that the discrete variable l_j is replaced by the continuous variable l, and we also made the further replacement

$$\sum_{j=-M}^{M} \to \frac{V}{(2\pi)^3} \int d^3 l \; .$$

The four-dimensional Eulerian frequency–wave-number spectrum associated with vertical displacement $S_{Es33}(k, \omega)$ can be obtained from Equation 7 and is given by

$$S_{Es33}(k, \omega) = \int \int C_{Es33}(X, \tau)$$

$$\times \exp[-i(k \cdot X - \omega\tau)] \, d\tau \, d^3 X$$

$$= \frac{\pi k_h^2 \Lambda_E(k)}{\rho k^2 \Omega^2(k)} \{ \delta[\Omega(k) - \omega]$$

$$+ \delta[\Omega(k) + \omega] \} \; . \qquad (8)$$

Finally, the three-dimensional Eulerian wave-number spectrum associated with vertical displacement can be obtained from Equation 8 and is given by

$$\hat{S}_{Es33}(k) = \frac{1}{2\pi} \int S_{Es33}(k, \omega) \, d\omega = \frac{k_h^2 \Lambda_E(k)}{\rho k^2 \Omega^2(k)} \; . \qquad (9)$$

The delta functions in Equation 8 confine the system to the dispersion surface described by $\Omega(k)$ so that the system is wavelike. The distribution of energy as a function of wave vector k is described by $\Lambda_E(k)$, and, as

previously noted, this is the quantity, or its equivalent, that is empirically specified by GM. Once $\Lambda_E(k)$ has been specified, Equation 8 can be used to compute any of the various one-dimensional marginal spectra required for a comparison with experiment. For example, the moored Eulerian vertical-displacement spectrum is given by

$$MS_{Es33}(\omega) = \int C_{Es33}(X = 0, \tau)\exp(i\omega\tau)\,d\tau$$

$$= \frac{1}{(2\pi)^3}\int S_{Es33}(k, \omega)\,d^3k \, , \qquad (10)$$

and the horizontal tow spectrum is given by

$$HTS_{Es33}(\kappa) = \int C_{Es33}(X_1, X_2 = X_3 = 0, \tau = 0)$$

$$\times \exp(-i\kappa X_1)\,dX_1$$

$$= \frac{1}{(2\pi)^3}$$

$$\times \int\int\int S_{Es33}(k_1 = \kappa, k_2\,k_3, \omega)$$

$$\times d\omega\,dk_2\,dk_3 \, . \qquad (11)$$

A variety of other correlation functions, coherences, and spectra (e.g., moored horizontal velocity spectrum, towed vertical coherence) can be calculated similarly. In all cases, the results depend on the distribution $\Lambda_E(k)$. The crux of the GM procedure is first to assume that the observed fields are due to linear internal waves and then to adjust $\Lambda_E(k)$ to obtain agreement among a wide variety of calculated statistical quantities, such as those given by Equations 10 and 11, and the corresponding experiments. The ability to obtain agreement supports the assumption that observed fields are at least partially due to linear internal waves. Such a procedure is entirely empirical, however, and does not provide a physical explanation for the particular choice of $\Lambda_E(k)$. Others[9,10] have attempted to provide an explanation but have ignored the difference between Lagrangian and Eulerian variables; as a consequence, we believe, they have not been particularly successful. In the treatment we provide here, it is important to realize that although $\Lambda_E(k)$ is referred to as the GM energy distribution, it actually describes the distribution of the Eulerian amplitudes a_{jm} and b_{jm}. We will show that this distribution may or may not, depending upon conditions, be the same as the energy distribution studied in statistical mechanics. Recognizing the difference will be important in obtaining a fundamental theory.

LAGRANGIAN VARIABLES

The Lagrangian displacement and velocity are written in the form

$$s_L(r, t) = \sum_{j=-M}^{M} \frac{1}{(2V\rho\Omega_j)^{1/2}}$$

$$\times \left[\left(\frac{l_{jh}}{l_j}\,\hat{r}_3 - \frac{l_{j3}}{l_j}\,\hat{l}_{jh}\right) q_j(t) - \frac{fl_{j3}}{\Omega_j l_j}\,\hat{n}_j p_j(t)\right]$$

$$\times \exp(il_j \cdot r) \, , \qquad (12a)$$

and

$$v_L(r, t) = \sum_{j=-M}^{M} \frac{1}{(2V\rho\Omega_j)^{1/2}}$$

$$\times \left[\left(\frac{l_{jh}}{l_j}\,\hat{r}_3 - \frac{l_{j3}}{l_j}\,\hat{l}_{jh}\right) \Omega_j p_j(t) + \frac{fl_{j3}}{l_j}\,\hat{n}_j q_j(t)\right]$$

$$\times \exp(il_j \cdot r) \, , \qquad (12b)$$

where $q_j(t)$ is a complex generalized displacement, $p_j(t)$ is the corresponding canonically conjugate momentum, and $\hat{r}_3 = \hat{x}_3$ is a vertical unit vector. The other parameters in Equations 12a and 12b are the same as in Equation 1. By using Equations 12a and 12b, it can be shown that the Hamiltonian (energy function) takes the form

$$H(p, q) = \sum_{j=-M}^{M} \frac{1}{4}\,\Omega_j(|p_j(t)|^2 + |q_j(t)|^2)$$

$$+ V_I(p, q)$$

$$= \sum_{j=1}^{M} \sum_{m=1}^{2} \frac{1}{2}\,\Omega_j[p_{jm}^2(t) + q_{jm}^2(t)]$$

$$+ V_I(p, q) \, . \qquad (13)$$

In the second expression of Equation 13, we have written the complex displacements and momenta in terms of their real and imaginary parts such that $q_j(t) = q_{j1}(t) + iq_{j2}(t)$ and $p_j(t) = p_{j1}(t) + ip_{j2}(t)$; thus, $q_{jm}(t)$ and $p_{jm}(t)$ $(1 \le j \le M, 1 \le m \le 2)$ are real, independent, canonically conjugate dynamical variables. In Equation 13, we have also written the Hamiltonian as a sum of two parts. The first part, which we will refer to as the free-field Hamiltonian, is quadratic in the dynamical variables and leads to linear equations of motion. The second part, $V_I(p, q)$, which we will refer to as the interaction potential, is of cubic and higher order in the dynamical variables and describes the nonlinear

352

interactions. Although we have used the eigenfunctions associated with linear internal waves in Equation 12, they have only been used as a convenient set of functions in terms of which to expand the displacement and velocity. As long as we retain the interaction potential $V_I(p, q)$, the description is fully nonlinear. A completely general case also has modes for which the quadratic part of the Hamiltonian is not of the harmonic oscillator type given in Equation 13. For example, the translational modes (sometimes called geostrophic or vortical modes) are of the free-particle type that require

$$\bar{H}(\bar{p}, \bar{q}) = \sum_{j=1}^{M} \sum_{m=1}^{2} C_j \bar{p}_{jm}^2(t) + \bar{V}_I(\bar{p}, \bar{q}) ,$$

where the overbars denote translational modes and C_j is a constant. The formulation can and eventually should be generalized to include these translational modes, but for now we will neglect them. This neglect ignores some potentially important issues concerning the diffusion of fluid parcels, but it is adequate for our purposes here.

The Lagrangian equations of motion are obtained by using the Hamiltonian given by Equation 13 in Hamilton's canonical equations to obtain

$$\dot{q}_{jm}(t) = \frac{\partial H(p, q)}{\partial p_{jm}(t)} = \Omega_j p_{jm}(t) + \frac{\partial V_I(p, q)}{\partial p_{jm}(t)} ,$$

(14a)

and

$$\dot{p}_{jm}(t) = -\frac{\partial H(p, q)}{\partial q_{jm}(t)} = -\Omega_j q_{jm}(t) - \frac{\partial V_I(p, q)}{\partial q_{jm}(t)} ,$$

(14b)

where the overdots denote differentiation with respect to time. In a general case, the equations of motion given by Equations 14a and 14b are nonlinear and cannot be solved exactly. The linear approximation is obtained by setting $V_I(p, q) = 0$, in which case it is easy to show that

$$q_{jm}(t + \tau) = q_{jm}(t)\cos(\Omega_j\tau) + p_{jm}(t)\sin(\Omega_j\tau) ,$$

(15a)

and

$$p_{jm}(t + \tau) = p_{jm}(t)\cos(\Omega_j\tau) - q_{jm}(t)\sin(\Omega_j\tau) ,$$

(15b)

where $p_{jm}(t)$ and $q_{jm}(t)$ are initial values that we have chosen to reference to time t rather than to zero for future convenience. For large many-body systems, the precise specification of the initial values is not possible, and

we must resort to statistical methods. Dealing with the nonlinear interactions requires perturbation or other approximation techniques. We will refer to the nonlinear interactions that arise from $V_I(p, q)$ as dynamic nonlinearities. Even though they can sometimes be treated as weak, these interactions play an important role in the time evolution of the relevant statistical quantities.

Although Equations 1 and 12a are formally identical, they are different in important and somewhat subtle ways. For disturbances that are small enough for all nonlinear interactions to be neglected, we can set $a_j(t) = q_j(t)$ and $b_j(t) = p_j(t)$. In this case, the Lagrangian and Eulerian descriptions are the same. It is important to realize, however, that the nonlinear terms associated with the two sets of variables are different. The dynamic nonlinearities also contribute to the Eulerian equations of motion, but because individual fluid parcels are continually flowing into and out of the region of interest, an additional nonlinear flow term, $(v_E \cdot \nabla)v_E$, must be considered. We will call this term the advective nonlinearity. Thus, for larger-amplitude disturbances, the two sets of variables cannot be equated, and the transformation between them becomes intractable. The two types of nonlinearities are fundamentally different. The dynamic nonlinearities are associated with the details of the forces between collections of fluid parcels, whereas the advective nonlinearity is associated with the flow of fluid parcels into and out of a fixed region of space and is strictly a Eulerian-frame concept. From a Lagrangian-frame point of view, the advective nonlinearity is a kinematic effect.

Independent of one's choice of variables, Lagrangian or Eulerian, this problem is inherently nonlinear. If all nonlinear interactions were neglected, then Lagrangian and Eulerian variables would be the same, and the linear internal-wave modes would not interact. This would mean that we could specify the initial amplitudes $p_{jm}(t)$ and $q_{jm}(t)$ at any convenient initial time t, and Equation 15 would be valid for all later times. This would also mean that any initial assignment of energy to a given mode would remain forever because no mechanism allows energy to be redistributed among the modes. Thus, nonlinear interactions must be present if the system is to evolve to a stationary state described by some statistical distribution, such as that given by Equation 4. On the other hand, because the nonlinear interactions for Lagrangian and Eulerian variables are different, we must expect that, in general, the statistical distribution of the Eulerian amplitudes will be different from the statistical distribution of the canonically conjugate Lagrangian variables. In statistical mechanics, the statistical distribution of the canonically conjugate Lagrangian variables is usually studied. For example, Prigogine[11] introduced the phase-space density function $g_L(p, q, t)$ that satisfies the Liouville equation and used perturbation methods to study the long-time evolution. By assuming that the nonlinear interactions were weak and by making the random phase assumption as an initial condition only, Prigogine obtained a master equation and showed that its long-time solution is of the Gaussian form given by

$$g_L(p, q, t) = \prod_{j=1}^{M} \prod_{m=1}^{2} \frac{\Omega_j}{2\pi\Lambda_{Lj}}$$

$$\times \exp\left[-\frac{\Omega_j}{2\Lambda_{Lj}} (p_{jm}^2 + q_{jm}^2) \right] , (16)$$

where we have suppressed explicit display of the reference time t, but it is to be understood that the p_{jm} and q_{jm} are evaluated at t. Although the form of Equation 16 is identical to that of Equation 4, the two expressions describe the distribution of different sets of variables. The phase-space density function given by Equation 16 describes the distribution of the canonically conjugate variables p_{jm} and q_{jm}, and Λ_{Lj} is the Lagrangian energy distribution that, in general, is different from the Eulerian distribution Λ_{Ej}.

The essence of the Prigogine treatment is that weak nonlinear interactions will redistribute energy among the linear modes such that starting from a wide variety of initial conditions, the system will, after a sufficiently long time t, evolve to a state that is described statistically by Equation 16. For relatively short times τ, we may treat the time evolution as linear and use the approximation given by Equation 15. Thus, we can use Equations 12, 15, and 16 to compute the various correlation functions and spectra. Because the form of the Lagrangian displacement given by Equation 12a is identical to that for the Eulerian displacement given by Equation 1, and because the forms of the probability density functions given by Equations 4 and 16 are identical, the calculation of the four-dimensional Lagrangian frequency–wave-number spectrum $S_{Ls33}(k, \omega)$ is the same as that for the corresponding Eulerian spectrum. We can write

$$S_{Ls33}(k, \omega) = \frac{\pi k_h^2 \Lambda_L(k)}{\rho k^2 \Omega^2(k)} \{\delta[\Omega(k) - \omega]$$

$$+ \delta[\Omega(k) + \omega]\} , (17)$$

where we have again allowed the volume of the ocean to become arbitrarily large. The three-dimensional Lagrangian wave-number spectrum is found as in Equation 9 to be

$$\hat{S}_{Ls33}(k) = \frac{k_h^2 \Lambda_L(k)}{\rho k^2 \Omega^2(k)} . (18)$$

The forms of Equations 17 and 18 are identical to those for the corresponding Eulerian quantities given by Equations 8 and 9, except for the replacement of $\Lambda_E(k)$ by $\Lambda_L(k)$. This difference, however slight it may seem, is crucial to understanding the relationship between the energy distributions studied in statistical mechanics and the observed oceanic spectra such as those given by Equations 10 and 11. The observed spectra are usually obtained from the Eulerian frequency–wave-number spectrum $\hat{S}_{Es33}(k)$ via Equations 10 and 11, whereas the

Lagrangian frequency–wave-number spectrum $\hat{S}_{Ls33}(k)$ is directly related to the distributions studied in statistical mechanics. Later we will obtain an expression for $\hat{S}_{Es33}(k)$ in terms of the various $\hat{S}_{Ls\alpha\beta}(k)$ and show that, in general, the two types of spectra are significantly different. This difference plays a key role in obtaining a first-principles explanation for the observed oceanic spectra.

Equations 17 and 18 show that the Lagrangian energy distribution $\Lambda_L(k)$ plays a crucial role in our description of the various Lagrangian spectra. In principle, it should be possible to derive $\Lambda_L(k)$ from a knowledge of the system interactions. Although this derivation is an ultimate goal and is important for a full understanding of the underlying physics, it is beyond our present capabilities. We can, however, determine some qualitative features of $\Lambda_L(k)$ and show that they can provide at least a partial understanding of the observed spectra. Our treatment in this article has made important use of the weak interaction approximation, both through the use of Equation 12 for short-time evolution and through the use of Equation 16 for the phase-space density function. We now need to consider in more detail the conditions for the validity of the weak-interaction approximation. The Hamiltonian given by Equation 13 can also be written in the form $H(p, q) = T(p, q) + V(p, q)$, where $T(p, q)$ is the kinetic energy and $V(p, q)$ is the full potential energy. The potential energy can be written in the form

$$V(p, q) = V_0(p, q) + V_1(p, q) = \int U(p, q, r) \, d^3r , (19)$$

where $V_0(p, q)$ denotes the quadratic part of the potential energy and $U(p, q, r)$ is the full potential energy density. The term $U(p, q, r)$ is a density in terms of the Lagrangian label r and must be expressed in terms of Lagrangian variables. The potential energy density for a vertically stratified compressible fluid is given by

$$U = P(z + s_{L3})J(s_L) - P(z) - \frac{\partial P(z)}{\partial z} s_{L3}$$

$$+ \frac{P(z)}{\gamma - 1} \left[\frac{1}{J(s_L)^{\gamma-1}} - 1 \right] , (20)$$

where we have assumed that expansion and compression of the fluid take place adiabatically. In Equation 20, the display of the dynamical variables (p, q) is suppressed, $J(s_L)$ is the Jacobian determinant associated with s_L (see Equation 28 for a concise definition), $P(z)$ is the static pressure at the vertical position z, and γ is the ratio of the specific heat at constant pressure to the specific heat at constant volume. For the static or undisturbed condition, $s_L = 0$; thus, the Lagrangian label r and the Eulerian label x are equal, and $z = r_3 = x_3$ is the vertical component of either the Lagrangian or the Eulerian label.

354

The form of the interaction potential required in Equation 13 is obtained by expanding the term $P(z + s_{L3})$ in Equation 20 about $s_{L3} = 0$ and the term $1/J(s_L)^{\gamma-1}$ about $J(s_L) = 1$. The quadratic terms are included in $V_0(p, q)$, whereas the cubic and higher-order terms are included in the interaction potential $V_1(p, q)$. By making the expansion, the quadratic part of the potential energy density U_0 is found to be

$$U_0 = \frac{\rho(z)}{2} \{[N^2(z) + g^2/c^2(z)]s_{L3}^2$$

$$+ c^2(z)(\nabla \cdot s_L)^2 - 2gs_{L3}\nabla \cdot s_L\} \ , \quad (21)$$

where $\rho(z)$ is the static fluid density, $N(z)$ is the Väisälä profile defined by

$$N^2(z) = -g\left[\frac{1}{\rho(z)}\frac{\partial\rho(z)}{\partial z} + \frac{g}{c^2(z)}\right] \ , \quad (22)$$

g is the acceleration due to gravity, $c(z)$ is the speed of sound defined by $c^2(z) = \gamma P(z)/\rho(z)$, and we have used the fundamental law of hydrostatics, which is given by $\partial P(z)/\partial z = -g\rho(z)$. A full treatment of Equation 21 yields internal waves, surface waves, sound, and the translational modes discussed earlier. The formulation presented here includes only internal waves. The theory can be generalized to include the additional modes, but for now we are concerned only with the internal waves. For the expansion given in Equation 13 to converge, we must limit both the size of the vertical component of the displacement and the size of the various spatial derivatives of all components of the displacement. To achieve these limitations, we must limit not only the average energy per mode but also the modal bandwidth. If the modes are occupied out to arbitrarily small length scales, then both the free-field energy and the nonlinear contributions from the interaction potential will be arbitrarily large. It can be shown from Equation 20 that the nonlinear energy grows much more rapidly as a function of decreasing length scale than the free-field energy does. Thus, strong nonlinear interactions will ultimately limit the participation of small length scales.

The class of interactions just discussed will be referred to as internal interactions because they are present even when the system is isolated. Interactions with the outside world, such as those associated with sources and sinks of energy, will be referred to as external interactions. We will consider a hierarchy of three cases that correspond to progressively greater levels of excitation as well as different relative strengths of the internal and external interactions. To limit the modal bandwidth, we will consider that molecular viscosity provides an absolute lower bound to the participation of the small-scale modes. In a typical situation, the modes that correspond to length scales shorter than about a millimeter are strongly damped and thus are ineffective for storing energy. We can, therefore, think of a minimum lower bound

μ_m (i.e., μ_m is on the order of 1 mm) for the length-scale cutoff provided by molecular viscosity. Although we will find, for internal waves, that processes other than molecular viscosity ultimately limit the participation of the small-scale modes, defining an absolute lower bound for the participating length scales is important in providing a framework within which to visualize the problem. The first case, which is the simplest and best known, is that for which the external interactions are negligible (i.e., the input and dissipation of energy are negligible) and the level of excitation is small enough to consider all internal nonlinear interactions as weak. In this case, energy is redistributed among the linear modes by weak internal interactions until the system reaches equilibrium, at which point energy is equipartitioned across the accessible modes. The second case is that for which the time scales associated with external interactions (i.e., energy input and dissipation) are comparable to or shorter than those associated with internal interactions, and the level of excitation, although greater than for the first case, is still small enough to treat the internal interactions as weak. The third case is that for which the internal interactions dominate, so that the time scales associated with internal interactions are shorter than those associated with external interactions and are important at length scales that are much greater than those associated with molecular viscosity. We now consider these three cases in greater detail.

We will find it convenient to write the average energy per mode in the form

$$\Lambda_{Lj} = E_0 h_j \ , \quad (23)$$

where E_0 is the maximum average energy per mode and h_j is a dimensionless (convergence) factor that provides the structure of the modal occupation and, more importantly, cuts off the participation of the modes that correspond to small length scales. If, for example, we consider a system for which the internal interactions dominate, then we would expect the system to evolve near to canonical equilibrium so that the phase-space density function is given by Equation 16, with $\Lambda_{Lj} = E_0$ and the number of degrees of freedom limited to length scales greater than μ_m by molecular viscosity. In this case, the convergence factor h_j is unity for modes that correspond to length scales greater than μ_m and then decreases rapidly to zero for modes that correspond to length scales smaller than μ_m. We must restrict E_0 to be small enough to assure that the nonlinear contributions are negligible, but if this condition is met, then Equation 16 can be used for the calculation of statistical averages. We will refer to this situation as case I.

If we now consider a system for which external interactions dominate, then we would expect the phase-space density function given by Equation 16, where Λ_{Lj} must be such that the modes excluded by molecular viscosity are not populated, but otherwise it is determined by external interactions that provide a heat bath (i.e., energy input and dissipation). In this case, the heat bath provides a horizontal length-scale cutoff μ_h and a vertical length-scale cutoff μ_v. Our use of the word cutoff does

not necessarily imply an abrupt cutoff. For example, the convergence factor h_j might be such that it exhibits a strong power-law decay for modes that correspond to horizontal length scales smaller than μ_h and vertical length scales smaller than μ_v. This situation is thought to be appropriate by most of the oceanographic community. In the usual oceanographic treatment of this problem,[12] the difference between Lagrangian and Eulerian variables is ignored, and it is assumed that generation and dissipation mechanisms provide a heat bath that establishes the convergence factor h_j such that the GM action spectrum is obtained. Even if the difference between Lagrangian and Eulerian variables were negligible, such a proposal simply transfers our lack of understanding to the heat bath, the detailed nature of which must be explained eventually. In the case of oceanic internal waves, the precise details of generation and dissipation mechanisms are not completely known, but what is known does not explain the quasi-universal character of the GM spectrum. Further, existing estimates of the evolution rates due to internal and external interactions suggest that at most length scales of interest, the internal interaction rates are much larger than the external interaction rates. Although this proposal has some attractive features, it does not resolve some important issues. We will refer to this situation as case II.

A third situation, which is the most intriguing, is also the most speculative. We now consider a system that is near canonical equilibrium but for which we cannot make the weak interaction approximation. In this case, the phase-space density function is given by

$$g(p, q) = \frac{1}{Z} \exp\left[- \frac{H(p, q)}{E_0} \right] , \qquad (24)$$

where Z is the partition function (i.e., normalization factor), $H(p, q)$ is the full Hamiltonian so that

$$\frac{H(p, q)}{E_0} = \sum_{j=1}^{M} \sum_{m=1}^{2} [(\Omega_j/2)(p_{jm}^2 + q_{jm}^2)$$

$$+ V_{1jm}(p, q)]/E_0$$

$$= \sum_{j=1}^{M} \sum_{m=1}^{2} (\Omega_j/2)(p_{jm}^2 + q_{jm}^2)$$

$$\times \frac{1 + V_{1jm}(p, q)/H_{0jm}(p, q)}{E_0} , \quad (25)$$

$H_{0jm}(p, q) = (\Omega_j/2)(p_{jm}^2 + q_{jm}^2)$, and we have written the interaction potential as a sum over modes. We can now define an effective energy for the jth mode $\hat{\Lambda}_{jm}(p, q)$ such that

$$\hat{\Lambda}_{jm}(p, q) = \frac{E_0}{1 + V_{1jm}(p, q)/H_{0jm}(p, q)} , \quad (26)$$

and write the phase-space density function in a form that looks similar to Equation 16. An important difference exists, however, between $\hat{\Lambda}_{jm}(p, q)$ and the average energy of the jth mode Λ_{Lj} in Equation 16. The parameter Λ_{Lj} does not depend on p_{jm} and q_{jm}, whereas $\hat{\Lambda}_{jm}(p, q)$ does. Obviously, Equation 24 is, in general, non-Gaussian, and no amount of manipulation can change this. If the nonlinear interaction energy associated with a given mode is small relative to the free-field energy associated with that mode, however, then Equation 26 yields approximately the constant E_0. On the other hand, if the nonlinear interaction energy associated with a given mode is much larger than the free-field energy associated with that mode, then Equation 26 yields a result much smaller than E_0, and because of the form of Equation 24, these modes are much less likely to be occupied. We have approximated this situation by replacing Equation 26 with an average value that is independent of p_{jm} and q_{jm} and assumed that the average rapidly approaches zero for length scales that are smaller than μ_h or μ_v. Such an approximation is qualitatively reasonable but cannot be expected to provide detailed quantitative information about the exclusion of the small-scale modes. If it were our goal to obtain precise information about the three-dimensional Lagrangian wave-number spectrum that is directly proportional to $\Lambda_L(k)$, then this shortcoming would be serious. We will find, however, that the various Eulerian spectra as well as the marginal Lagrangian spectra associated with moored measurements are not sensitive to these details, and, therefore, this approximation is adequate for our purposes here. We will refer to this situation as case III. The cutoff proposed in case III is equivalent to arguments concerning the breakdown of internal waves due to local instabilities at small Richardson number.[8]

EULERIAN VARIABLES

The relation between Lagrangian and Eulerian variables is established by the definition

$$s_{E3}(x, t) = \int s_{L3}(r, t)\delta[x - r - s_L(r, t)]$$

$$\times J[s_L(r, t)] \, d^3r , \qquad (27)$$

where the Jacobian determinant $J(s_L)$ is given by

$$J(s_L) = \sum_{\alpha=1}^{3} \sum_{\beta=1}^{3} \sum_{\gamma=1}^{3} \epsilon_{\alpha\beta\gamma} \left(\delta_{1\alpha} - \frac{\partial s_{L1}}{\partial r_\alpha} \right)$$

$$\times \left(\delta_{2\beta} - \frac{\partial s_{L2}}{\partial r_\beta} \right) \left(\delta_{3\gamma} - \frac{\partial s_{L3}}{\partial r_\gamma} \right) , \quad (28)$$

and $\epsilon_{\alpha\beta\gamma}$ is the perfectly antisymmetric unit tensor of the third rank. Equation 27 is a well-known relation[13-15] that can be used to express any Eulerian variable [e.g., $v_{E\alpha}(x, t)$] in terms of Lagrangian variables.

To gain a better understanding of Equation 27, we make the transformation $y = r + s_L(r, t)$ and note that $J[s_L(r, t)]d^3r = d^3y$, so that Equation 27 can be evaluated to yield

$$s_E(x, t) = s_L(r, t) , \qquad (29)$$

where

$$x = r + s_L(r, t) . \qquad (30)$$

The expressions given by Equations 29 and 30 constitute the usual relation between Lagrangian and Eulerian variables.[8,16]

Although Equations 29 and 30 appear to be simple, they actually disguise a complicated procedure. The difficulty is that implementing Equation 29 as a point transformation requires Equation 30 to be inverted to obtain r as a function of x and, for all but trivially simple Lagrangian displacement fields, that inversion is intractable. An important recent contribution[5,6] was the recognition that even though Equation 27 does not generate a useful exact point relationship, it can be used for calculating statistical averages and leads to entirely tractable expressions. The key to achieving this result is to write the delta function in Equation 27 in terms of its Fourier transform so that

$$\delta[x - r - s_L(r, t)] = \frac{1}{(2\pi)^3}$$

$$\times \int \exp\{im \cdot [x - r - s_L(r, t)]\} \, d^3m , \qquad (31)$$

where m is the Fourier transform variable.

If we now use Equations 27 and 31 and use the phase-space density function given by Equation 16 to compute the Eulerian displacement correlation function, then the need to invert Equation 30 is avoided and a complicated but tractable expression is obtained.

The details of the following calculations are given in a recent publication,[5] henceforth referred to as AJ. By using Equation 12a to express the displacements in terms of the canonically conjugate dynamical variables and by approximating the time evolution for relatively short times τ by Equation 15, it is shown in AJ that the Eulerian correlation function $C_{Es33}(X, \tau)$ is given by

$$C_{Es33}(X, \tau) = E[s_{E3}(x + X, t + \tau)s_{E3}(x, t)]$$

$$= \frac{1}{(2\pi)^3} \int \int M_{33}(R, \tau, m)$$

$$\times \exp[im \cdot (X - R)] \, d^3m \, d^3R , \qquad (32)$$

where

$$M_{33}(R, \tau, m) = E[s_{L3}(r, t)s_{L3}(r', t')$$

$$\times J[s_L(r, t)]J[s_L(r', t')]$$

$$\times \exp\{im \cdot [s_L(r, t) - s_L(r', t')]\}] , \qquad (33)$$

$R = r - r'$, and $\tau = t - t'$. The four-dimensional Eulerian frequency–wave-number spectrum is found from Equation 32 to be

$$S_{Es33}(k, \omega) = \int \int C_{Es33}(X, \tau)$$

$$\times \exp(ik \cdot X - \omega\tau) \, d\tau \, d^3X$$

$$= \int \int M_{33}(R, \tau, k)$$

$$\times \exp(ik \cdot R - \omega\tau) \, d\tau \, d^3R . \quad (34)$$

The expression for the frequency–wave-number spectrum given by Equation 34 is a central result. Its practical utility, however, depends on obtaining a tractable expression for the function $M_{33}(R, k, \tau)$ defined by Equation 33. If the phase-space density function is of the Gaussian form given by Equation 16, then by using the procedure described in AJ, it is always possible to obtain an exact expression for $M_{33}(R, k, \tau)$. Although the calculations given in AJ are straightforward, they are lengthy, and the final expression for $M_{33}(R, k, \tau)$ is complicated. Fortunately, examining all of the details of that result is not necessary to discuss the important features of the Eulerian spectra. We will make no attempt to provide complete calculations, choosing instead to refer to AJ for details and only quote results in this article. It is shown in AJ that the frequency–wave-number spectrum given by Equation 34 exhibits different properties depending on the wave numbers involved. The first wave-number regime corresponds to small wave numbers and is defined by requiring that

$$(\nu_h^2 k_h^2 + \nu_v^2 k_3^2) << 1 , \qquad (35)$$

where ν_h and ν_v are the root-mean-square horizontal and vertical Lagrangian displacements. If all of the k_α are small enough to assure that the expression given by Equation 35 is satisfied, then it is shown in AJ that

$$S_{Es33}(k, \omega) \approx S_{Ls33}(k, \omega) . \qquad (36)$$

We thus find that for wave numbers that are small enough to assure that Equation 35 is satisfied, the Eulerian and Lagrangian frequency–wave-number spectra are approximately equal.

The opposite extreme is the case for which at least one of the k_α is large enough to assure that

$$1 << (\nu_h^2 k_h^2 + \nu_v^2 k_3^2) . \tag{37}$$

In this case, it is shown in AJ that

$$S_{Es33}(k, \omega) \approx \left(\frac{\pi}{\eta_h^2 k_h^2 + \eta_v^2 k_3^2} \right)^{\frac{1}{2}}$$

$$\times \exp\left[\frac{-\omega^2}{4(\eta_h^2 k_h^2 + \eta_v^2 k_3^2)} \right] \frac{\Psi(\hat{k})}{k^5} , \tag{38}$$

where η_h and η_v are the root-mean-square horizontal and vertical Lagrangian velocities and $\hat{k}$ is a unit vector in the direction of k. An explicit expression for $\Psi(\hat{k})$ is given in AJ, but for our purposes here, it is only important to note that $\Psi(\hat{k})$ depends on the direction of k but not on its magnitude. It follows directly from Equation 38 that for large k, the four-dimensional Eulerian frequency–wave-number spectrum decays as $1/k^6$. Further, unlike the corresponding Lagrangian frequency–wave-number spectrum given by Equation 17, the Eulerian frequency–wave-number spectrum is not proportional to the delta functions that confine the system to the dispersion surface. Thus, from an Eulerian-frame point of view, at large wave numbers, the dispersion surface is completely smeared and the system is not wavelike. We have found that at small wave numbers, the Eulerian and Lagrangian frequency–wave-number spectra are approximately equal. At larger wave numbers, the Eulerian frequency–wave-number spectrum decays as $1/k^6$, whereas the Lagrangian frequency–wave-number spectrum decays as the the convergence factor $h(k)$ (see Equation 23). Most importantly, Equation 38 is independent of the detailed nature of $h(k)$. Thus, whereas the Lagrangian spectra (see Equations 17 and 18) are directly sensitive to the details of $h(k)$, the corresponding Eulerian spectra are not.

Some of the one-dimensional marginal spectra, such as the frequency spectra and moored coherences discussed in the last section, are obtained by integrating over all wave numbers. In the case of both Lagrangian and Eulerian spectra, such integrals are dominated by contributions from small k_α where the Eulerian and Lagrangian frequency–wave-number spectra are approximately equal. Hence, the one-dimensional Eulerian frequency spectra and coherences are approximately equal to the corresponding Lagrangian spectra and coherences. The horizontal tow spectrum, on the other hand, is an Eulerian spectrum and presents a different situation. It can be obtained from the frequency–wave-number spectrum given by Equation 34 by integrating over ω, setting $k_1 = \kappa$, and integrating over k_2 and k_3. For small κ such that the product $\kappa\nu_h$ is somewhat less than unity, the integrals are dominated by small values of k_2 and k_3 so that the Eulerian tow spectrum is approximately equal to the one-dimensional Lagrangian horizon-

tal wave-number spectrum. For larger κ such that the product $\kappa\nu_h$ is somewhat larger than unity, the expression for the frequency–wave-number spectrum given by Equation 38 is appropriate and a significantly different result is obtained. By setting $k_1 = \kappa$ and integrating Equation 38 over ω, k_2, and k_3, it can be shown that

$$HTS_{Es33}(\kappa) = \frac{W}{\kappa^3} , \tag{39}$$

where an expression for W, which depends on N, f, E_0, μ_h, and μ_v, is given in AJ. We have thus found that the one-dimensional Eulerian horizontal tow spectrum is equal to the Lagrangian horizontal tow spectrum at small κ and decays as κ^{-3} at large κ.

DISCUSSION

We first consider the case of the moored spectrum shown in Figure 1 and compare it with the Lagrangian frequency spectrum, which can be computed from Equation 17. Although the moored spectra measured in some experiments are in terms of Eulerian variables and in others are in terms of Lagrangian variables, it is shown in AJ that the moored spectra are dominated by small wave numbers where the two types of spectra are approximately equal. Thus, a comparison with the Lagrangian frequency spectrum for all types of moored experiments is appropriate. To obtain an explicit expression for the moored frequency spectrum $MS_{Ls33}(\omega)$, we must specify an explicit expression for the convergence factor $h(k)$. For this purpose, we have taken $h(k) = \exp[-\frac{1}{2}(\mu_h^2 k_h^2 + \mu_v^2 k_3^2)]$. It is shown in AJ that the moored spectra are insensitive to the details of $h(k)$, and that the only important feature is the introduction of the two length scales μ_h and μ_v, at which the contributions from small horizontal and vertical length scales are suppressed. The Gaussian form for $h(k)$ is for mathematical convenience only, and any other choice that introduces length-scale cutoffs will produce essentially the same results. The expression just given for $h(k)$ can be used in Equation 17 to obtain an expression for $MS_{Ls33}(\omega)$ that is in excellent agreement with experiment at all frequencies except those very near the spectral cutoff at N. The disagreement near N is due to our use of periodic boundary conditions in the vertical direction, and replacing these with a clamped surface-boundary condition yields excellent agreement with experiment at all frequencies. An expression for $MS_{Ls33}(\omega)$ that employs a clamped surface-boundary condition and depends on the parameters E_0/ρ, μ_h, μ_v, N, f, and the depth r_3 is obtained in AJ. In the following comparison, the values of N, f, and r_3 are chosen to correspond to the particular experiment under consideration, and we have adjusted the parameters E_0/ρ, μ_h, and μ_v to obtain a reasonable comparison. It is shown in AJ that the assumed values for these parameters are consistent with the situation referred to as case III. In Figure 3, the black curve is a plot of the moored vertical displacement spectrum given in AJ where, for the purpose of this plot, we have chosen $\mu_h = 700$ m, $\mu_v =$
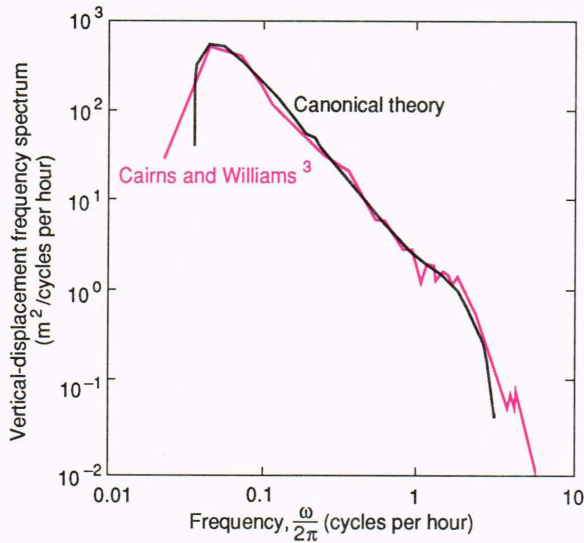
Figure 3. A comparison between theory and experiment for a typical moored vertical-displacement spectrum. (Adapted from Ref. 3.)

Figure 4. A comparison between theory and experiment for a typical vertical-displacement horizontal tow spectrum. (Adapted from Ref. 4.)

7 m, $E_0/\rho = 1.2 \times 10^5$ J · m³/kg, $r_3 = 350$ m, $N = 3.2$ cycles per hour, and $f = 0.035$ cycles per hour. The red curve in Figure 3 is the Cairns and Williams result[3] shown earlier in Figure 1. The excellent qualitative agreement is obvious.

We now consider an example of a tow spectrum. The tow spectra are always Eulerian and mostly at wave numbers for which the Eulerian and Lagrangian spectra are different. The example we consider is the horizontal tow spectrum $HTS_{Es33}(\kappa)$ given by Equation 39, which was found at large wave numbers to decay as κ^{-3}. This decay is similar to that observed experimentally and is independent of the detailed nature of the Lagrangian convergence factor. The red curve in Figure 4 is a plot of the horizontal tow spectrum given by Equation 39, where W was calculated in AJ [we again use the Gaussian form for $h(k)$], and for the purpose of this plot, we have chosen $E_0/\rho = 1.4 \times 10^5$ J · m³/kg, $\mu_h = 700$ m, $\mu_v = 7$ m, $r_3 = 700$ m, $N = 2.5$ cycles per hour, and $f = 0.035$ cycles per hour. The blue curve is the $\kappa = 0$ limit of the Lagrangian horizontal tow spectrum obtained from Equation 18, which is approximately the level of the Eulerian horizontal tow spectrum at small κ. The points plotted as a scattergram in Figure 4 are the Katz results[4] shown earlier in Figure 2. This plot is typical of towed measurements. Although the agreement between our theoretical result and experiment is not perfect, the qualitative similarity is apparent. We have not computed the theoretical Eulerian spectrum for wavelengths between 1 and 10 km because a numerical integration would be required since these wavelengths are not in either asymptotic region. Near 1 km, however, the red curve breaks to a smaller slope and finally merges with the blue curve at approximately 10 km. A noticeable difference between our theory and experiment occurs at very small wave numbers (i.e., near the blue curve in Figure 4) where the Lagrangian and Eulerian spectra are approximately equal. This difference may indicate a departure from canonical
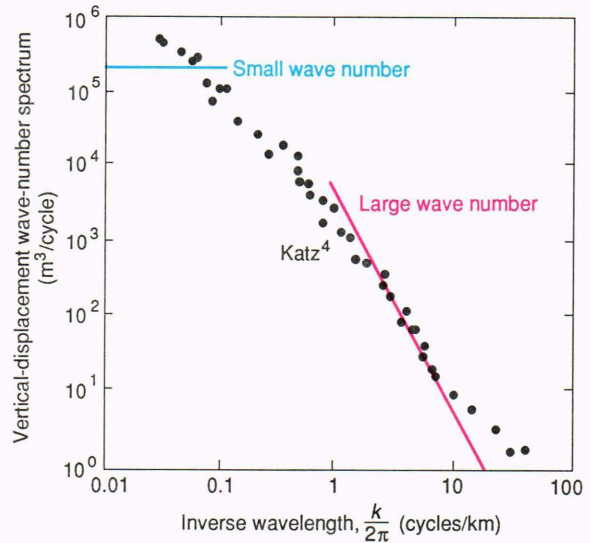
equilibrium at small wave numbers. Such a departure would not be surprising, because source contributions are thought to be strong at these small wave numbers. Overall, the agreement obtained is excellent, and the values of the parameters used in generating Figure 4 are nearly the same as those used in generating Figure 3. This situation demonstrates consistency between two significantly different experiments and shows that the values used in generating both figures are completely reasonable.

A more extensive comparison between theory and experiment is given in AJ, and the additional comparisons are just as favorable as those shown in Figures 3 and 4. By considering the strength of the dynamic nonlinear interactions, it is also shown in AJ that all of the values of the various parameters required to obtain a favorable comparison with experiment are consistent with the situation we have referred to as case III. Although our comparison with experiment has tended to emphasize canonical equilibrium via case III, the more important result is our relation between Eulerian and Lagrangian spectra and the demonstration that the two can be significantly different. None of the marginal Eulerian spectra that are usually measured are very sensitive to the details of the underlying Lagrangian spectra. Thus, the Lagrangian spectra may differ considerably from canonical equilibrium and still result in Eulerian spectra that are entirely similar to those obtained from case III. The fundamental dynamical processes directly affect the Lagrangian spectra but are masked in the Eulerian spectra by the advective tail. Experiments that focus on this advective Eulerian tail cannot yield information about the fundamental dynamical processes.

We wish to emphasize that all existing tow measurements are Eulerian and consequently provide detailed information about the advective tail only. Our results show that the advective tail is devoid of information about the fundamental dynamical processes. Experiments that obtain Lagrangian information are required for studying

these fundamental dynamical processes. Lagrangian measurements are fluid-parcel following measurements, and this feature is important if we are to retain a direct correspondence with the particles of Newtonian mechanics. An example of a Lagrangian measurement is a dye measurement with coded dye or a dye measurement performed in conjunction with vertical temperature measurements. In addition, other experiments might be suggested; clearly, some measurement that explores this issue is critically needed.

Another interesting and potentially important result is that the four-dimensional Eulerian frequency–wavenumber spectrum is not confined to the dispersion surface. As far as we know, no experimental evidence concerning this issue exists. The Doppler sonar observations of Pinkel[17] are a step in this direction but have yielded only two-dimensional frequency–wave-number spectra. Because the two-dimensional spectra are obtained by integrating over two components of the three-dimensional wave vector, information concerning the existence of delta functions (i.e., sharp peaks) that confine the system to the dispersion surface is lost. Our expressions can be used to compute theoretical expressions to be compared with Pinkel's results. Although such a comparison would certainly be interesting and the calculations are tractable, they are also nontrivial and have yet to be completed.

Although the Eulerian spectra are insensitive to the details of the convergence factor $h(k)$, the length scales μ_h and μ_v play an important role. So far we have treated these scales as adjustable. In principle, it should be possible to compute them from a detailed knowledge of the nonlinear interactions once the level E_0 has been specified. Such an investigation is important for a full understanding of the physics, but it is beyond the scope of our considerations in this article. It has not been our intent to present this work as a *fait accompli*. Rather, we have sought to present only enough evidence to support a reasonable argument in favor of case III and, more importantly, to elucidate the differences between Lagrangian and Eulerian spectra. Many important, and we believe fruitful, investigations remain to be done, including a more detailed investigation of strong nonlinear interactions within the Lagrangian frame and the role they play in establishing the length scales μ_h and μ_v. Further, as noted previously, we have neglected the translational modes. By so doing, we have ignored possible alterations to the spectra in regions with substantial mean currents, as well as some potentially important issues concerning diffusion. The methods we have introduced here can also include the translational modes and thus can be considered for a variety of additional investigations.

Although the emphasis in this article has been on internal waves, the methods and major conclusions are also applicable to surface waves and possibly even to some aspects of atmospheric motions. Our major point is that for any of these systems, the fundamental dynamical processes are easier to describe in terms of Lagrangian variables, but most measurements are easier to describe in terms of Eulerian variables. The two sets of variables are different, but the consequences of their differences have not been adequately considered. This work has shown that significant differences between Lagrangian and Eulerian statistical quantities can exist and that care must be taken to distinguish between the two types of variables. Concepts such as nonlinear transition rates and the role they play in the approach to equilibrium, which have been extensively studied in statistical mechanics in terms of Lagrangian variables, do not lead directly to explanations for the shapes of the various empirical Eulerian spectra. To obtain the agreement illustrated in Figures 3 and 4, we had to distinguish carefully between Lagrangian and Eulerian variables and account in detail for the effects of advection. We introduced a theoretical procedure that enables us to deal with this problem and is applicable to various physical systems.

REFERENCES

[1] Garrett, C. J. R., and Munk, W. H., "Space–Time Scales of Internal Waves," *Geophys. Fluid Dyn.* **3**, 225–264 (1972).
[2] Garrett, C. J. R., and Munk, W. H., "Space–Time Scales of Internal Waves: A Progress Report," *J. Geophys. Res.* **80**, 291–297 (1975).
[3] Cairns, J. L., and Williams, G. O., "Internal Wave Observations from a Midwater Float, 2," *J. Geophys. Res.* **81**, 1943–1950 (1976).
[4] Katz, E. J., "Tow Spectra from MODE," *J. Geophys. Res.* **80**, 1163–1167 (1975).
[5] Allen, K. R., and Joseph, R. I., "A Canonical Statistical Theory of Oceanic Internal Waves," *J. Fluid Mech.* **204**, 185–228 (1989).
[6] Allen, K. R., and Joseph, R. I., "The Relation Between Lagrangian and Eulerian Spectra Based upon a Canonical Statistical Theory of Geophysical Fluid Waves," *Phys. Rev. A* **39**, 5243–5257 (1989).
[7] Tolstoy, I., "The Theory of Waves in Stratified Fluids Including the Effects of Gravity and Rotation," *Rev. Mod. Phys.* **35**, 207–230 (1963).
[8] Phillips, O. M., *The Dynamics of the Upper Ocean*, Cambridge Univ. Press, London (1969).
[9] Holloway, G., "Theoretical Approaches to Interactions Among Internal Waves, Turbulence, and Finestructure," in *AIP Conf. Proc. No. 76*, West, B. J., ed., American Institute of Physics, New York, pp. 47–77 (1981).
[10] Pomphrey, N., "Review of Some Calculations of Energy Transport in a Garrett–Munk Ocean," in *AIP Conf. Proc. No. 76*, West, B. J., ed., American Institute of Physics, New York, pp. 113–128 (1981).
[11] Prigogine, I., *Non-Equilibrium Statistical Mechanics*, Interscience, New York (1962).
[12] McComas, C. H., and Müller, P., "The Dynamic Balance of Internal Waves," *J. Phys. Oceanogr.* **11**, 970–986 (1981).
[13] Hardy, R. J., "Energy-Flux Operator for a Lattice," *Phys. Rev.* **132**, 168–177 (1963).
[14] Mori, H., Oppenheim, I., and Ross, J., "Some Topics in Quantum Statistics: The Wigner Function and Transport Theory," in *Studies in Statistical Mechanics*, DeBoer, J., and Uhlenbeck, G. E., eds., Interscience, New York, Vol. I, pp. 271–298 (1962).
[15] Abarbanel, H. D. I., and Rouhi, A., "Phase Space Density Representation of Inviscid Fluid Dynamics," *Phys. Fluids* **30**, 2952–2964 (1987).
[16] Lamb, H., *Hydrodynamics*, Dover, New York (1945).
[17] Pinkel, R., "Doppler Sonar Observations of Internal Waves: The Wavenumber–Frequency Spectrum," *J. Phys. Oceanogr.* **14**, 1249–1270 (1984).

THE AUTHORS

KENNETH R. ALLEN received B.S., M.S., and Ph.D. degrees in theoretical physics from the Georgia Institute of Technology in 1961, 1964, and 1967, respectively. From 1967 to 1973, he was Assistant Professor of Physics at the University of Florida. From 1974 to 1979, he was Senior Research Physicist and Head of the Physics Division at the Naval Coastal Systems Center in Panama City, Fla. From 1979 to 1981, he was Senior Research Physicist at Dynamics Technology in Torrance, Calif. Dr. Allen joined APL in 1981 and is a member of the Principal Professional Staff in the Submarine Technology Department and a lecturer at The Johns Hopkins University G.W.C. Whiting School of Engineering.
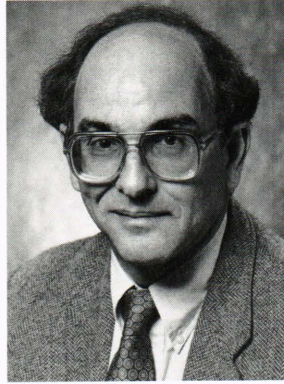
RICHARD I. JOSEPH received a B.S. from the City College of the City University of New York in 1957 and a Ph.D. from Harvard University in 1962, both in physics. From 1961 to 1966, he was a senior scientist with the Research Division of the Raytheon Co. Since 1966, Dr. Joseph has been with the Department of Electrical and Computer Engineering of The Johns Hopkins University, where he is currently the Jacob Suter Jammer Professor of Electrical and Computer Engineering, and he is a member of APL's Principal Professional Staff. During 1972, Dr. Joseph was a Visiting Professor of Physics at the Kings College, University of London, on a Guggenheim Fellowship, and he is a Fellow of the American Physical Society.